To appear in ApJ Letter

Searching for dark matter halos in the Suprime-Cam 2 sq deg field

Satoshi Miyazaki[1,7], Takashi Hamana[1], Kazuhiro Shimasaku[2], Hisanori Furusawa[1], Mamoru Doi[3], Masaru Hamabe[4], Katsumi Imi[5], Masahiko Kimura[6], Yutaka Komiyama[1], Fumiaki Nakata[1], Norio Okada[1], Sadanori Okamura[2], Masami Ouchi[2], Maki Sekiguchi[6], Masafumi Yagi[1] and Naoki Yasuda[1,7]

ABSTRACT

We report the first result of weak gravitational lensing survey on a 2.1 deg^2 R_c-band image taken with a wide field camera (Suprime-Cam) on the prime focus of 8.2 m Subaru Telescope. The weak lensing mass reconstruction is applied to the data to search for dark matter halos of cluster scale; $M \geq 10^{14} M_\odot$. The reconstructed convergence field is divided by 1-σ noise to obtain the signal-to-noise ratio map (S/N-map) of the detection. Local maxima and minima are searched on the S/N-map and the probability distribution function (PDF) of the peaks are created to compare with model predictions. We found excess over noise PDF created from the randomized realization on both positive and negative sides. Negative peaks imply the presence of voids in the dark matter distribution and this is the first report of the detection. Positive peaks, on the other hand, represent the dark matter halos and the number count of the halos on the 2.1 deg^2 image is 4.9 ± 2.3 for S/N > 5 where the Gaussian smoothing radius of the convergence map is $1'$. The result is consistent with the prediction assuming the Press-Schechter mass function and the NFW halo profile under the cluster normalized CDM cosmology. Although the present statistics is not

---

[1]National Astronomical Observatory of Japan, Mitaka, Tokyo 181-8588, Japan

[2]Department of Astronomy, University of Tokyo, Bunkyo, Tokyo 113-0033, Japan

[3]Institute of Astronomy, University of Tokyo, Mitaka, Tokyo 181-0015, Japan

[4]Department of Mathematical and Physical Sciences,Japan Women's University, Bunkyo, Tokyo 112-8681, Japan

[5]Communication Network Center (Tsu-den) , Mitsubishi Electric, Amagasaki, Hyogo 661-8661, Japan

[6]Institute for Cosmic Ray Research, University of Tokyo, Kashiwa,Chiba 277-8582, Japan

[7]The Graduate University for Advanced Studies (Sokendai)

enough because of the limited field of view, this work demonstrates that dark matter halo count via weak lensing is a promising way to test the paradigm of structure formation and cosmological model.

Subject headings: cosmology: observations—dark matter—large scale structure of universe—gravitational lensing

1. Introduction

Dark matter halos, which are the virialized systems formed via the gravitational amplification of initial density fluctuations, are one of the most important cosmological probes. Since their evolution is governed purely by gravity, their number density and the evolution of clustering properties can be precisely predicted analytically as well as numerically. Weak lensing is a unique observational technique to detect dark matter halos because it detects halos not by their *light* but by more essential physical parameter, the *mass*. It also allows us to directly estimate the halo mass bypassing a use of ambiguous empirical relations like the mass-temperature (or velocity dispersion) or mass-luminosity relations. Therefore, comparison of theories and weak lensing observations is a direct and reliable way to test the paradigm of the structure formation and to constrain the cosmological parameters.

Theoretical prescriptions for predicting statistics of weak lensing halos have been developed so far. Kruse & Schneider (1999) first calculated the expected number of dark matter halos detected by means of the aperture mass method (Schneider 1996). Predicted number density of halos exceeds 10 per deg^2 for cluster-normalized cosmologies if one obtains moderately deep images whose galaxy density is n_g ∼30 arcmin^{-2}. Bartelmann et al. (2001) pointed out that the number density is sensitive to the density profile of halos. On the other hand, Jain & van Waerbeke (2000) discussed the statistics of the *peaks* on convergence map. They claimed that the statistics can be an alternative approach to probe the mass function of dark matter halos and to constrain Ω_m.

Observationally, weak lensing has become reliable measures to map the dark matter distribution in clusters of galaxies (see a review by Mellier 1999). Recently, serendipitous detections of mass concentrations outside clusters on a reconstructed mass map have been reported by several authors (Erben et al. 2000; Umetsu & Futamase 2000; Wittman et al. 2001; Miralles et al. 2002). All cases have no clear optical counterparts except the one by Wittman et al. (2001) which is identified as a cluster of galaxies at $z = 0.276$.

These findings demonstrate that dark matter halo search via weak lensing is feasible and can detect even lower luminosity dark matter halos that are overlooked in conventional optical cluster surveys. The number of samples obtained so far is, however, limited. In order to make statistically significant discussions, weak lensing survey over a representative cosmic volume is crucial. The survey requires not only wide field but also high image quality to make reliable lensing analysis. Suprime-Cam on the 8 m Subaru telescope is the most ideal camera for the purpose. The median seeing in I_c band monitored over a year and a half is reported to be $\sim$ 0.6 arcsec (Miyazaki et al. 2002). In this *Letter*, we report the first results from the Suprime-Cam weak lensing survey that covers contiguous 2.1 deg^2 field. We examine statistical properties of local peaks on the reconstructed convergence map by comparing with model predictions.

2. Observation and data reduction

We set field size at 2.1 deg^2, which is the largest size possible to be accomplished during the commissioning phase of the Suprime-Cam. The field we chose is centered at R.A. = $16^h04^m43^s$, decl. = +43°12'19" (J2000.0). In order to compare light and mass we observed one of the seven fields that Gunn et al. (1986) made cluster surveys (GHO survey). The 2.1 deg^2 field has twelve GHO clusters and one Abell cluster (A 2158). Note, however, that the number density of clusters in this field is comparable to the one averaged over the seven GHO fields.

We obtained R_c-band images on the nights of 2001 April 23-25. Suprime-Cam provides a field of view of 34'$\times$ 27' with a scale 0".202 pixel^{-1}. Nine contiguous fields were observed in 3$\times$3 mosaic configuration. Each exposure on a given field was offset by 1' from other exposures to remove cosmic rays and defects on the CCDs. Total exposure time on each field was 1800 sec (360 sec $\times$ 5).

The individual images were de-biased and then flattened using a median of all object frames taken during the observing run. Registration on each field was first performed assuming a simple geometrical model. The parameters of the model include (1) optical distortion, (2) displacement and rotation of each CCD from the fiducial position and (3) the offset of pointing between the exposures (Miyazaki et al. 2002). These parameters can be solved by minimizing position errors of control stars common to all exposures and used for the first transformation of the images to a common coordinate system. After the transformation, the residual of the position of the control stars is $\sim$ 0.5 pixel rms. The residual is due to several effects not considered in the simple model including atmospheric dispersion and asymmetric aberration of optics. We note, however, that the residual vector is smoothly changing over position and can be well modeled as the third order bi-linear polynomial function of position. This model then gives the fine correction of the transformation function. As a result the final residual decreased typically down to 0.07 pixel rms (14 miliarcsec). The seeing in the resulting image is 0".68 FWHM and the scatter among the fields is quite small at 0".04 rms.

We used the software suite *imcat*, an actual implementation of Kaiser et al. (1995), to carry out object detection, photometry and shape measurements of objects. Catalogs created for the nine fields are registered using stars on overlapping regions to result in a final catalog whose total field of view is $1.64^\circ \times 1.28^\circ$. Differences in photometric zero point among the fields due to variation of sky condition were compensated at this stage but the adjustment was not significant (~ 0.05 mag). For weak lensing analysis, we adopt galaxies of $22 < R < 25.5$ whose signal-to-noise (S/N) ratio, nu, calculated in the imcat exceeds 15 (Bacon et al. 2001). The number of objects in the catalog is 297547 (39.3 arcmin^{-2}) and the count peaks at R = 25.2.

3. Galaxy shape analysis

The estimate of the shear, $\vec{\gamma}$, from the observed ellipticities of galaxies, $\vec{e} = \{I_{11} - I_{22}, 2I_{12}\}/(I_{11} + I_{22})$ involves two steps where I_{ij} are quadrupole moments of the surface brightness of objects. First, PSF anisotropy is corrected using the image of stars as references,

$$\vec{e'} = \vec{e} - \frac{P_{sm}}{P^*_{sm}}\vec{e^*}, \tag{1}$$

where P_{sm} is the smear polarisability tensors and is mostly diagonal (Kaiser et al. 1995). $(P^*_{sm})^{-1}\vec{e^*}$ was calculated for stars scattered over the field of view and we made fifth order bi-polynomial fit to the values as a function of the positions. This function is used in Eqn.(1) to correct the ellipticities of faint galaxies. The nine fields are treated independently in this procedure. The rms value of ellipticities of the reference stars, $\langle|\vec{e^*}|^2\rangle^{\frac{1}{2}}$, is reduced from 2.7% to 1.3% as a result of the correction. Note that the rms before the correction is already small thanks to the superb image quality of Subaru telescope.

Luppino & Kaiser (1997) worked out how to correct the ellipticities for the effect of the seeing. The *pre*-seeing shear $\vec{\gamma}$ is described as

$$\vec{\gamma} = P_\gamma^{-1}\vec{e'}, \quad P_\gamma = P_{sh} - \frac{P^*_{sh}}{P^*_{sm}}P_{sm}, \tag{2}$$

where P_{sh} is the shear polarisability tensor. The P_γ of individual galaxies are, however, known to be noisy estimate and we thus adopted smoothing and weighting method developed by van Waerbeke et al.(2000; see also Erben et al. 2001 for a detail study of the smoothing scheme). For each object, twenty neighbors are first identified in the r_g-*magnitude* plane where r_g is a measure of size of objects which the *imcat* yields. A median value of P_γ among the neighbors is adopted for a smoothed P_γ of the object. The variance of raw γ before the smoothing among the neighbors, σ_γ^2, is used to estimate the weight of the object, w_n, as $w_n = 1/(\sigma_\gamma^2 + \alpha^2)$ where α^2 is the variance of all the objects in the catalog and $\alpha \simeq 0.4$ here. Under the weighting scheme, an averaged value of a certain observable, $\langle Q \rangle$, is calculated as $\sum_{i=1}^N w_{n,i} Q_i / \sum_{i=1}^N w_{n,i}$ instead of $\sum_{i=1}^N Q_i/N$. The $\langle \mathrm{tr}(P_\gamma) \rangle$ for all objects is calculated as 0.31 but P_γ depends on r_g. For objects with $r_g > 3.5$, $\langle \mathrm{tr}(P_\gamma) \rangle$ is almost constant, ~ 0.65, and becomes small below the r_g down to $\langle \mathrm{tr}(P_\gamma) \rangle \sim 0.2$ for $r_g = 1.5$.

4. Results and discussions

The convergence field, κ, is estimated using the original Kaiser & Squires (1993) inversion algorithm with a Gaussian window function $W(\theta) = \exp(-|\boldsymbol{\theta}|^2/\theta_G^2)/\pi\theta_G^2$. In order to estimate the noise of κ field, we randomized the orientations of the galaxies in the catalog and created a $\kappa_{\rm noise}$ map. The variance of the $\kappa_{\rm noise}$ depends on the smoothing scale θ_G and is represented as $\sigma_{\rm noise} \sim 0.023\theta_G^{-1}$. This turned out to be consistent with theoretical estimate,

$$\sigma_{\rm noise} = \frac{\sigma_\epsilon}{2\theta_G\sqrt{\pi n_g}}, \tag{3}$$

where $\sigma_\epsilon = 0.42$ and $n_g = 39.3 \mathrm{arcmin}^{-2}$ are the observed variance of galaxy ellipticities and number density, respectively, yielding $\sigma_{\rm noise} = 0.020\theta_G^{-1}$.

We repeated the randomization 100 times and compute the rms among them at each grid where κ is computed. Since κ is Gaussian in its errors, this rms represents 1-σ noise level on each grid, and thus the measured signal divided by the rms gives the S/N ratio, ν, at that grid. Thick contour in Fig. 1 shows the S/N-map with a smoothing scale of $\theta_G = 1'$. Threshold of the contour is set at 3.

One notes that numbers of dark halo candidates are detected. For reference, number density of moderately bright galaxies are super-imposed as thin contour. It is surprising that correlation of mass and light is clearly visible from this relatively simple analysis on the single band image. A halo that has the highest significance is designated (X) in Fig. 1. In this halo, the galaxy density also shows an excess as large as the other known clusters. In fact, a spectroscopic observation of two member galaxies implies that it is a cluster located at the redshift of 0.41. This object is not listed on the NASA/IPAC Extragalactic Database (NED). Other follow-up observations are underway and detailed comparison of mass and light will be discussed in subsequent papers.

Let us turn to statistical properties of the S/N-map, and we will compare the results with the model predictions. First, we examine the probability distribution function (PDF) of peaks. Peaks are identified by pixels having a higher or lower value of ν than the all eight surrounding pixels as suggested by Jain & van Waerbeke (2000). The PDF of the peak heights is shown as thick histograms of left two panels in Fig. 2. The thin histogram shows a noise PDF measured from $\kappa_{\rm noise}$ maps, the average of 100 randomizations is plotted and the error bars show the rms among them. The bimodal feature of the noise PDF is due to superposition of two contributions each of which is due to positive peaks and negative peaks (= troughs). Excess counts over the noise PDF is apparent on both positive ($\nu \geq 3$) and negative ($\nu \leq -3$) side of the histogram. The excess becomes more apparent as θ_G increases. The positive peaks imply the existence of dark matter halos whereas the natural explanation of the negative peaks seen is voids (Jain & van Waerbeke 2000). This is the first observational evidence of the existence of voids in the matter distribution revealed by weak lensing.

Right panels of Fig. 2 show the peak PDF measured from numerical experiments of the gravitational lensing by large-scale structures. The experiments were performed using the ray-tracing technique combined with large N-body simulations and its details are described in Ménard et al. (2002). Briefly, N-body data from Very Large simulation carried out by the Virgo Consortium (Jenkins et al 2001; Yoshida, Sheth & Diaferio 2001) were used to generate the dark matter distribution. A ΛCDM model ($\Omega_m = 0.3$, $\Omega_\lambda = 0.7$, $h = 0.7$ and $\sigma_8 = 0.9$) is assumed. The multiple-lens plane ray-tracing algorithm was used to follow the light rays (Hamana & Mellier 2001, see also Jain, Seljak & White 2000 for technical detail). The lensing convergence and shear were computed for 1024^2 pixels with the pixel size of 0.25 arcmin for a single source plane of $z_s = 1$. We generated the simulated noisy κ map following the procedure described in Jain & van Waerbeke (2000). The noise is modeled as a Gaussian random field with the variance measured in the real data. The peak is identified as the same manner as for the observed data. Ten realizations of the numerical experiment were used to compute the peak PDF (the total field size is 10×4.27^2 deg^2, much larger than the observed data, and thus the peak distribution is very smooth).

The simulated PDF is very similar to the observed PDF. Jain & van Waerbeke (2000) pointed out that the peak PDF can be used to discriminate the cosmological model. They demonstrated using the ray-tracing experiments of a high density ($\Omega_m = 1.0$, $\Omega_\lambda = 0$, $\sigma_8 = 0.9$) and a low density($\Omega_m = 0.3$, $\Omega_\lambda = 0$, $\sigma_8 = 0.9$) models that the high density model has broader distribution than the low density model, especially on the negative side. It should be noticed that they adopted $\sigma_\epsilon = 0.2$ which is about half of our measured value, therefore one should not directly compare our real PDFs with theirs (Figure 3 of Jain & van Waerbeke (2000)).

In addition to the limited statistics of this work, theoretical prescription of the peak PDF is, however, still premature for placing constraint on the cosmological model in a quantitative manner. We therefore concentrate here only on excess on the positive side; the halo number count. We calculated number of the positive peaks, N_{obs}, in the observed S/N map exceeding $\nu_{\rm th}$. Halo number count is defined as $N_{halo} = N_{obs} - N_r \pm \sqrt{N_{obs} + \sigma_{N_r}^2}$ where N_r and σ_{N_r} is average peak counts obtained on the randomized catalogs and their variances, respectively. The halo count is shown in Fig. 3 as well as theoretical predictions which are constructed following Kruse & Schneider (1999). We assumed a high positive peak in κ map comes from a single halo whose number density is described by Press-Schechter mass function (Press & Schechter 1974; we used its modified model by Sheth & Tormen 1999). We further assumed that all halos have a universal density profile that Navarro et al. (1996) proposed (NFW); $\rho(r) = \rho_s r^{-1}(1+r)^{-2}$. We also compared the results with another halo profile, singular isothermal sphere model (SIS); $\rho(r) = \rho_s r^{-2}$. For the relation between the scale length of the halo and halo mass we adopted the fitting form by Bullock et al (2001). The $\sigma_{\rm noise}$ measured from observed data is used to convert κ to ν. Note that Kruse & Schneider (1999) and Bartelmann et al. (2001) adopted $\sigma_\epsilon = 0.2$, thus their predicted count is much larger than our prediction.

First, if one considers only highly significant halos, say $\nu \geq 5$, the predicted halo number count does not depends strongly on the background cosmology as is presented in Fig.3, where dashed line and solid line shows the SCDM model ($\Omega_m = 1$, $\Omega_\Lambda = 0$, $\sigma_8 = 0.6$, $h = 0.5$) and ΛCDM ($\Omega_m = 0.3$, $\Omega_\Lambda = 0.7$, $\sigma_8 = 0.9$, $h = 0.7$), respectively. The count, however, depends on the halo profile; the SIS predicts fewer counts as is shown in the dotted line in the figure. The observed count prefers NFW profile although the poisson error in $\nu \geq 6$ is large in this work. It is demonstrated here that number count of highly significant halos can be an useful probe for the dark matter halo profile because of the independence of background cosmology. Meanwhile, the dependence becomes clearly visible in the counts of moderately significant haloes ($\nu < 5$); the SCDM predicts more counts than LCDM does due mainly to larger Ω_m. Our observed result shows high number counts which favors high density universe. This result, however, cannot be taken at face value since the large excess is apparent in Fig.2 as a spike around $\nu \sim 3.5$. Therefore, the excess count in the moderately significant halos is likely due to the cosmic variance. Comparison of data taken on multiple (say 5 to 10) uncorrelated fields of this size is necessary to evaluate the contribution from the cosmic variance and eventually to discuss cosmological models.

In summary, the present work clearly demonstrates that weak lensing technique is indeed a promising way to probe matter distribution purely through the mass. We detected not only the high positive peaks due to massive halos but also the excess in the peak PDF on the negative side which is the first observational evidence of the voids in dark matter distribution. Dark matter halo counts is proved to be the useful tool to test the paradigm of the structure formation and cosmological models. The cosmic variance that we encountered in this work should be evaluated by the data obtained by future high resolution wider field imaging survey.

We are grateful to L. van Waerbeke for helpful discussions about galaxy shape analysis, and M. Bartelmann for useful discussions. We thank Richard Ellis and Alexandre Refregier for their careful reading of the manuscript and the comments. T.H. F.N. and M.O. acknowledge support from Research Fellowships of the Japan Society for the Promotion of Science.

REFERENCES

Bacon, D.J., Refregier, A., Clowe, D. & Ellis, R.S. 2001, MNRAS, 325, 1065

Bartelmann, M., King, L.J. & Schneider, P. 2001 A&A, 378, 361

Bullock, J. S., Kolatt, T. S., Sigad, Y., Somerville, R. S., Kravtsov, A. V., Klypin, A. A., Primack, J. R., Dekel, A. 2001, MNRAS, 321, 559

Erben, T., van Waerbeke, L., Mellier, Y., Schneider, P., Cuillandre, J.-C., Castander, F.J. & Dantel-Fort, M. 2000 A&A, 355, 23

Erben, T., van Waerbeke, L., Bertin, E., Mellier, & Y. & Schneider, P. 2001, A&A, 366, 717

Gunn, J.E., Hoessel, J.G. & Oke, J.B. 1986, ApJ, 306, 30

Hamana, T. & Mellier, Y. 2001, MNRAS, 327, 169

Hamana, T., Colombi, S. T., Thion, A., Devriendt, J. E., Meller, Y., & Bernardeau, F. 2002, MNRAS, 330, 365

Jain, B. Seljak, U. & White, S. D. M. 2000, ApJ, 530, 547

Jain, B. & van Waerbeke, L. 2000, ApJ, 530, L1

Jenkins, A., Frenk, C. S., White, S. D. M., Colberg, J. M., Cole, S., Evrard, A. E., Couchman, H. M. P. & Yoshida, N. 2001, MNRAS, 321, 372

Kaiser, N. & Squires, G. 1993, ApJ, 404, 441

Kaiser, N., Squires, G. & Broadhurst, T. 1995, ApJ, 449, 460

Kruse, G. & Schneider, P. 1999 MNRAS, 302, 821

Luppino, G.A. & Kaiser, N. 1997, ApJ, 475, 20L

Mellier, Y. 1999 ARA&A, 37, 127

Ménard, B., Hamana, T., Bartelmann, M., & Yoshida, N., 2002, submitted to A&A (astro-ph/0210112)

Miralles, J.-M., Erben, T., Hämmerle, H., Schneider, P., Fosbury, R.A.E., Freudling, W., Pirzkal, N., Jain, B. & White, S.D.M. 2002, A&A, 388, 68

Miyazaki, S., Komiyama, Y., Sekiguchi, M., Okamura, S., Doi, M., Furusawa, H., Hamabe, M., Imi, K., Kimura, M., Nakata, F., Okada, N., Ouchi, M., Shimasaku, K., Yagi, M., Yasuda, N., & 2002, PASJin press

Navarro, J., Frenk, C. & White, S. 1996 ApJ, 462, 563

Press, W. & Schechter, P. 1974 ApJ, 185, 397

Schneider, P. 1996, MNRAS, 283, 837

Sheth, R. K., & Tormen, G. 1999, MNRAS, 308, 119

Umetsu, K. & Futamase, T. 2000, ApJ, 539, L5

Van Waerbeke, L., Mellier, Y., Erben, T. et al. 2000, A&A, 358, 30

Wittman, D.M., Tyson, J.A., Margonier, V.E., Cohen, J.G. & Dell'Antonio, I.P. 2001, ApJ, 557, L89

Yoshida, N., Sheth, R. K. & Diaferio, A. 2001, MNRAS, 328, 669

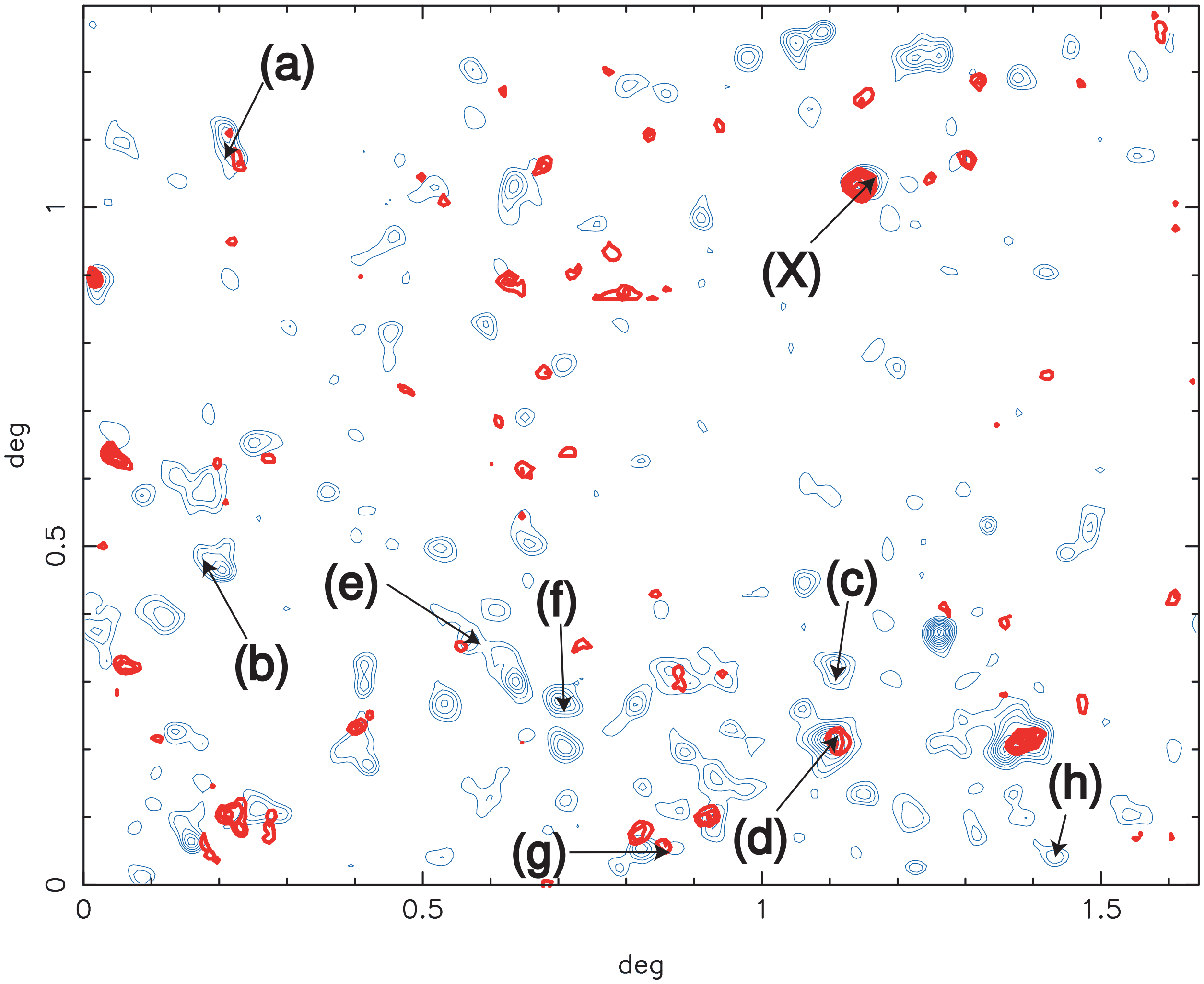

Fig. 1.— Red contour represents the signal to noise ratio (ν) of convergence field. Data of $\nu > 3$ is shown. Blue contour shows number density of moderately bright galaxies, $20 < R_c < 23$. Symbols (a)-(h) are designated where clusters listed in the NASA/IPAC Extragalactic Database (NED) are located and excess of galaxy number density is visible in the map; (a)GHO1606+4346, (b)Abell2158 (0.13), (c)GHO1601+4259 (0.54), (d)GHO1601+4253 (0.54), (e)GHO1604+4303, (f)GHO1603+4256, (g)GHO1602+4245, (h)GHO1559+4242. The redshift is shown in the bracket if known. Both maps are smoothed with Gaussian kernel of $\theta_G = 1'$.

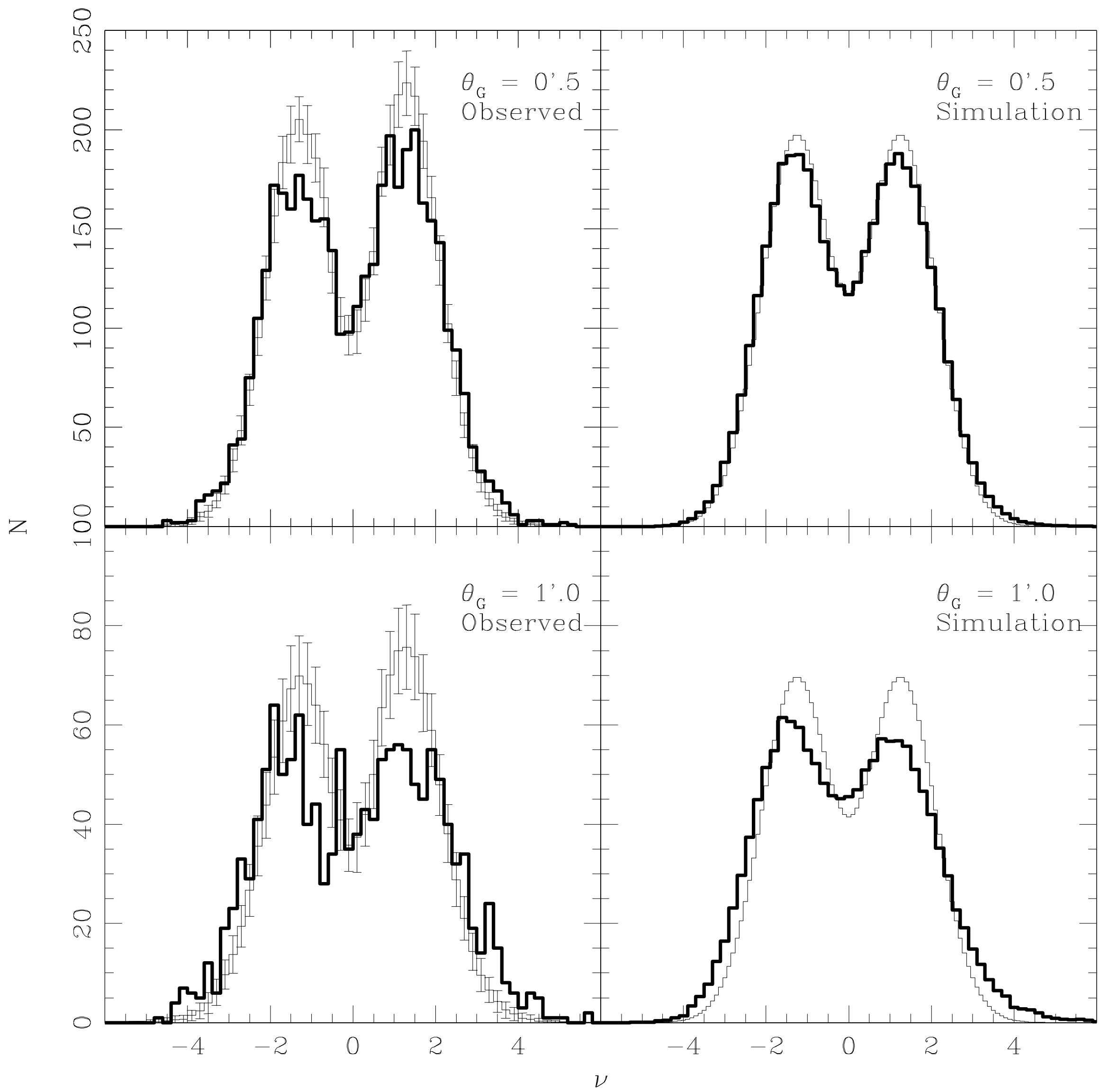

Fig. 2.— Peak distribution function in *kappa* map with smoothing scale $\theta_G = 0'.5$ (top) and $1'$ (bottom). Thick solid histograms on the left panels show the results obtained from the observed catalog and thin solid histograms associated with error bars are averaged results of 100 random realizations of galaxy orientation in the catalog. The errors are rms of the randomization. Results from ΛCDM model simulation are shown as thick histograms on the right based on the observed parameters, $\sigma_{noise} = 0.023\theta_G^{-1}$ assuming $z_s = 1.0$ and their pure noise PDF is shown as thin histograms.

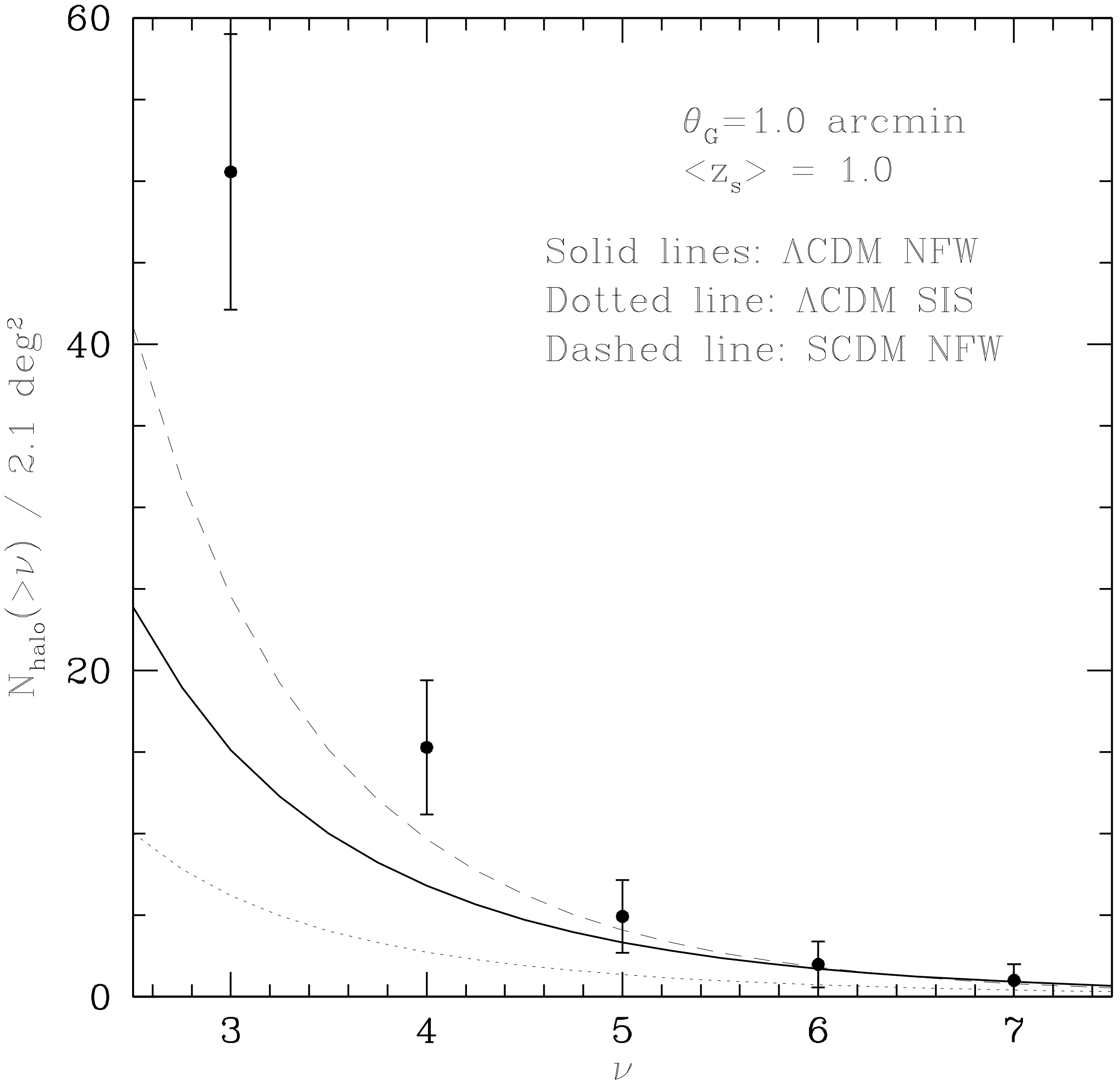

Fig. 3.— Dark matter halo counts on the convergence field with $\theta_G = 1'$. The counts due to noise are estimated from the random realizations and subtracted. Solid and dotted line show ΛCDM model with the halo profile of NFW and SIS, respectively. Dashed line presents SCDM with NFW profile. The model calculation assumes a single source redshift of $z_s = 1.0$. Broadening of the redshift distribution makes the count slightly less but the effect is a few percents at most as far as the empirical distribution with reasonable parameters are assumed (e.g. Hamana et al. 2002).